



# Case Study: Comparison of current QDMR practices and applicability of FRP technology

Report 2002-005-C-02

The research described in this report was carried out by

Project Leader	Dr. Sujeeva Setunge
Team members	Prof. Arun Kumar, Dr. Abe Nezamian and Dr Saman De Silva (RMIT) Dr. Alan Carse, Mr. John Spathonis and Ms. Louise Chandler (QDMR) Mr. Dale Gilbert (QDPW) Mr. Bruce Johnson (Ove Arup) Prof. Alan Jeary (UWS) Dr. Lam Pham (CSIRO)

Research Program C:  
Delivery and Management of Built Assets

Project 2002-005-C  
Decision Support Tools for Concrete Infrastructure rehabilitation

## Contents

<b>LIST OF TABLES .....</b>	<b>4</b>
<b>LIST OF FIGURES.....</b>	<b>4</b>
<b>EXECUTIVE SUMMARY .....</b>	<b>5</b>
<b>1 INTRODUCTION.....</b>	<b>6</b>
<b>2 DESCRIPTION OF THE CASE-STUDY: TENTHILL CREEK BRIDGE .....</b>	<b>8</b>
<b>2.1 Location .....</b>	<b>8</b>
<b>2.2 Details of the Bridge .....</b>	<b>8</b>
<b>2.3 Description of the Expected Freight .....</b>	<b>10</b>
<b>2.3.1 Explanation of the loads .....</b>	<b>11</b>
<b>2.3.1.1 Self-weight.....</b>	<b>11</b>
<b>2.3.1.2 Traffic loads.....</b>	<b>11</b>
<b>2.3.1.3 Thermal effects.....</b>	<b>11</b>
<b>2.3.1.4 Wind loads.....</b>	<b>11</b>
<b>2.3.1.5 Flood loads.....</b>	<b>11</b>
<b>2.3.2 Load combinations.....</b>	<b>12</b>
<b>2.3.2.1 Classification of loads and load effects .....</b>	<b>12</b>
<b>2.3.2.2 Load combination for serviceability limit state.....</b>	<b>12</b>
<b>2.3.2.3 Load combination for ultimate limit state .....</b>	<b>12</b>
<b>2.4 Observed damage to the headstock .....</b>	<b>13</b>
<b>3 EVALUATION OF THE EXISTING DESIGN ACTIONS ON THE BRIDGE HEADSTOCK.....</b>	<b>14</b>
<b>3.1 Structural Analysis of the Headstock .....</b>	<b>14</b>
<b>3.2 Maximum design bending moments and shear .....</b>	<b>15</b>
<b>4 CALCULATION OF THE EXISTING CAPACITY OF THE HEADSTOCK.....</b>	<b>17</b>
<b>4.1 Assumptions Relating to the Capacity Analysis .....</b>	<b>17</b>
<b>4.2 Residual Flexural Capacity of the Headstock .....</b>	<b>17</b>
<b>4.3 Residual capacity of the bridge headstock in shear .....</b>	<b>18</b>
<b>5 STRENGTHENING OF THE BRIDGE HEADSTOCK WITH EXTERNAL POST-TENSIONING .....</b>	<b>19</b>
<b>5.1 Design parameters.....</b>	<b>19</b>

<b>5.2</b>	<b>Structural calculations</b> .....	<b>19</b>
5.2.1	Shear capacity .....	19
5.2.1.1	Flexural-shear cracking .....	19
5.2.1.2	Web shear cracking .....	20
5.2.2	Flexural capacity.....	21
<b>6</b>	<b>STRENGTHENING OF THE BRIDGE HEADSTOCK USING FRP COMPOSITES</b> .....	<b>22</b>
6.1	Background .....	22
6.2	Design Guidelines.....	22
6.3	Design of FRP System.....	22
6.4	Flexural Strengthening.....	23
6.4.1	Design material properties.....	24
6.4.2	Initial situation .....	24
6.4.3	Capacity of the strengthened beam .....	25
6.4.4	Anchorage.....	28
6.5	Shear strengthening .....	31
6.6	Other issues .....	33
6.7	Comparison of the provisions of the two major guidelines: ACI and FIB .....	34
6.8	Summary of FRP strengthening scheme.....	34
<b>7</b>	<b>COMPARISON OF POST TENSIONING AND FRP STRENGTHENING</b> .....	<b>37</b>
7.1	Flexural Strengthening.....	37
7.2	Shear Strengthening.....	37
7.3	Conclusions .....	38
<b>8</b>	<b>CONCLUSIONS</b> .....	<b>39</b>
<b>9</b>	<b>REFERENCES</b> .....	<b>41</b>
<b>10.</b>	<b>NOTATION</b> .....	<b>42</b>
<b>11.</b>	<b>AUTHOR BIOGRAPHIES</b> .....	<b>45</b>

**LIST OF TABLES**

*Table 6-1 Material properties of FRP systems.....* 23

*Table 6-2 Design material properties complying with the FIB guideline.....* 24

*Table 6-3 Design material properties according to the ACI guideline.....* 24

**LIST OF FIGURES**

*Figure 2-1: Location of Tenthill bridge .....* 8

*Figure 2-2 Photos of the Tenthill Bridge .....* 9

*Figure 2-3: Schematic details of the headstock .....* 10

*Figure 2-4: Section details of a longitudinal pre-stressed beam .....* 10

*Figure 2-5: Observed cracks in the headstock.....* 13

*Figure 3-1 Applied dead load on the headstock.....* 15

*Figure 4-1: Beam section of headstock and internal strain stress distribution .....* 17

*Figure 6-1 Idealised stress-strain curves for constitutive materials at ULS.....* 23

*Figure 6-2 Initial situation .....* 25

*Figure 6-3 Internal strain and stress distributions for the beam cross section of the headstock .....* 26

*Figure 6-4 Envelope line of the tensile forces .....* 30

*Figure 6-5 Flexural strengthening scheme .....* 35

*Figure 6-6 Shear strengthening scheme.....* 36

## **EXECUTIVE SUMMARY**

In the report 2002-005-C-01 the research team has compiled the state-of-the art of FRP technology, which can be used in structural strengthening of reinforced concrete bridges. This report covers assessment of current practices of QDMR through a case study. An innovative strengthening scheme is proposed for the bridge using FRP technology, which can be used as a basis for the development of a decision support tool for rehabilitation of reinforced concrete bridge structures using Fibre Reinforced Polymer composites. A comparison between the current practices and the innovative methodology is also covered by this document.

The case study considered herein is the reinforced concrete headstock of a three span reinforced and pre-stressed concrete bridge structure in Gatton, Queensland. Details of the bridge structure and the damage as assessed by the research team are detailed in this document.

The structures division of QDMR (Ms. Louise Chandler) has developed a solution for rehabilitation of the bridge structure using external post-tensioning. The research team has re-assessed the capacity of the existing structure through their own analysis and compared it with the solution by QDMR. The details of the calculations are given identifying the decisions taken at various stages of the design.

Subsequently, the research team has completed a new solution using Fibre Reinforced Polymer composites for strengthening of the bridge structure. The details of the calculations are given again identifying the decisions faced by the designer at various stages of the development of the solution.

# 1 INTRODUCTION

Rehabilitation and upgrading of existing civil engineering infrastructure has recently become a major issue which often requires immediate attention of asset managers. There are a number of situations where an increase in structural capacity of a structure in service will be required. These include change of use, new loading criteria, impact, damage and deterioration of material. Bridge structures are deteriorating at a fast rate, and cost for repair and replacement of deficient bridges are continuously rising. Even when resources are available, extended time is often required for performing needed remedies, causing distribution of traffic and inconvenience to the traveling public. The strengthening or retrofitting of existing concrete structures to resist higher design loads, correct deterioration-related damage, or increase ductility has traditionally been accomplished using conventional materials and construction techniques. Externally bonded steel plates, steel or concrete jackets and external post tensioning are just some of the many traditional techniques available. Recent developments in fiber reinforced polymer (FRP) composites have opened up another cost-efficient alternative for consideration of the asset managers.

Strength of FRP composites come largely from the fibers, which are usually glass, carbon, or aramid. FRP materials are lightweight, non-corrosive, non-magnetic and exhibit high tensile strength. Additionally, these materials are readily available in several forms ranging from factory made laminates to dry fiber sheets that can be wrapped to conform to the geometry of a structure before adding the polymer resin. The relatively thin profile of cured FRP systems is often desirable in applications where aesthetics or access is a concern (Nystrom et al. 2003).

Whilst there have been a number of reinforced concrete bridge girder strengthening projects completed in Australia using FRP materials, in each occasion, an overseas consulting company or an academic institution has been engaged to perform the structural design and consultancy advice (Kalra and Neubauer, 2003 and Shepherd and Sarkady 2002). Queensland Department of Main Roads has developed several innovative solutions in collaboration with the Fiber Composites centre at University of Southern Queensland for specific applications (Carse, 1996). However, these are most of the time one-off applications which did not lead to establishment of general guidelines for designing strengthening schemes using the innovative FRP systems.

This report covers a case study of strengthening of the deteriorated Tenthill creek bridge headstock in Queensland. As built design documents for the bridge has been reviewed in detail to understand the residual capacity of the bridge headstock and an on-site inspection has been conducted to identify the location and nature of the cracks. A traditional strengthening solution developed for the bridge using external post tensioning is presented identifying decisions taken by the designer at each stage.

An alternative strengthening scheme has been developed using FRP composites readily available in the Australian market place. The design has been conducted utilizing most up to date research information available as well as the two design guidelines available for the use of FRP composites for strengthening: The Design and Construction of Externally Bonded FRP Systems for Strengthening Concrete Structures reported by ACI Committee 440 and The Technical Report of Externally Bonded FRP Reinforcement for RC Structures (FIB 14). Design calculations for the strengthening of Tenthill bridge headstock using FRP composites is presented as a case study covering the provisions reported in research literature. Finally the report provides a comparison of the strengthening schemes using external post-tensioning and FRP composites as well as a comparison between the FRP solutions using the two overseas design guidelines.

The work completed herein sets the scene for identifying the major decisions a structural designer would face in selecting a structural strengthening scheme for a deteriorated reinforced concrete bridge structure using innovative materials and technologies.

## 2 DESCRIPTION OF THE CASE-STUDY: TENTHILL CREEK BRIDGE

The case study was selected after a number of discussions with QDMR and identifying that the headstock of reinforced and pre-stressed concrete bridge structures is currently the weak link, which requires strengthening to satisfy the current requirements of traffic and other loading.

### 2.1 Location

The bridge studied in this report was built in 1976 and used to carry a state highway of Ipswich-Toowoomba over Tenthill Creek in Gatton, Queensland, Australia. The bridge has now been bypassed by the 4 lanes Gatton Bypass. It is now on road 314 Gatton Clifton. The location of the bridge is shown in Figure 2-1.

Figure 2-1: Location of Tenthill bridge



### 2.2 Details of the Bridge

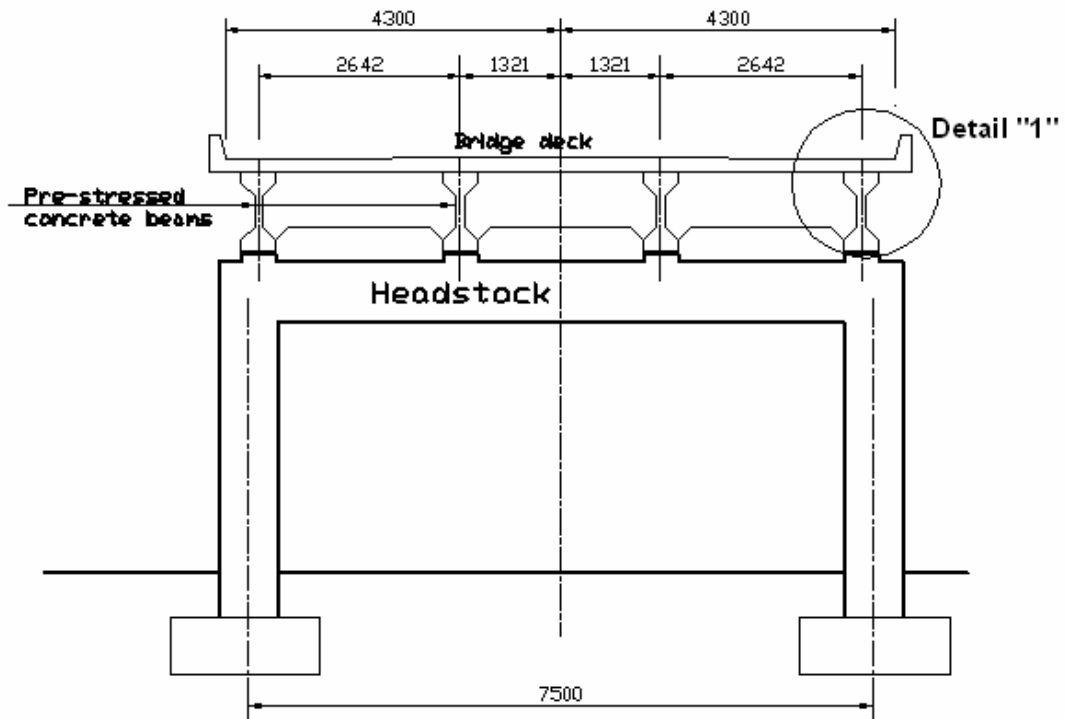
This simple span reinforced concrete, pre-stressed-beam structure was built in 1970's. The bridge is 82.15 m long and about 8.6 m wide and is supported by a total of 12 pre-stressed 27.38 m long beams over three spans of 27.38 m. Side and cross views of the Tenthill Bridge are shown in Figure 2-2. The beams are supported by two abutments and two headstocks. A headstock elevation view is shown in Figure 2-3.



*Figure 2-2 Photos of the Tenthill Bridge*

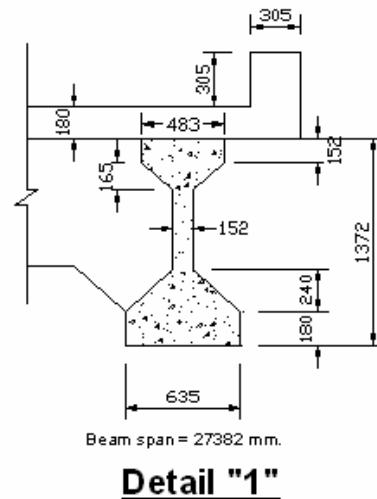


Figure 2-3: Schematic details of the headstock



The section details of a typical pre-stressed concrete beam is shown in Figure 2-4

Figure 2-4: Section details of a longitudinal pre-stressed beam



## 2.3 Description of the Expected Freight

Austrroads bridge design code (1992) was used for assessment of the bridge to ascertain the capacity of the bridge. The Ipswich-Toowoomba road over Tenthill Creek is selected as

functional Class 3 from the Table 2.3.4 of Austroads code (1992). The possible application of loads and load effects on the bridge can be categorized as follows:

- Permanent effects  
Including structure selfweight, superimposed dead loads, loads due to normal water flow etc.
- Thermal effects  
Including effects due to changes in temperature.
- Transient effects  
Including traffic loading, wind loads, flood loads, debris and impact loads, earthquakes loads.

### **2.3.1 Explanation of the loads**

#### **2.3.1.1 Self-weight**

The self-weight is the weight of the structural parts and the non structural parts of the bridge which are not subjected to changes during the construction and the usage of the bridge. The design dead loads for serviceability and ultimate states have been calculated by multiplying the nominal dead loads by load factors from Austroad Bridge code, Table 2.2.2.

#### **2.3.1.2 Traffic loads**

The loading due to vehicles or pedestrians is the traffic loads. As illustrated in Austroads Code, the traffic loads on a bridge can be represented by T44 truck loading, L44 lane loading, heavy load platform loading and W7 wheel loading. In the bridge design it is not required to use vehicle traffic loading and pedestrian loading at the same time. The traffic loading models of T44 and HLP 300 have been used for analysis and design of the headstock strengthening system. To obtain the traffic design loads for Serviceability and Ultimate states, the nominal traffic loads were multiplied by load factors and dynamic load allowances in accordance with Austroad Bridge design code clause 2.3.11, clause 2.4 , Table 2.3.11 and Figure 2.4.2.

#### **2.3.1.3 Thermal effects**

Thermal effects can be due to the varying average bridge temperature and also due to different temperature gradients in structural members of the bridge. Variations in the design loads or the load effects due to expansion or contraction of the form of structure or the support should be considered. The longitudinal beams of the bridge are designed as simply supported beams; hence, the thermal effect from the longitudinal beams can be ignored. Due to the relatively small length of headstock, the thermal effect on the headstock was not included in analysis of the headstock.

#### **2.3.1.4 Wind loads**

Due to the weight of the concrete bridge, the wind loads can be ignored in analysis and design of the headstock strengthening system.

#### **2.3.1.5 Flood loads**

If a bridge is to be constructed over a river, it has to be designed by considering the effects due to water flow. Further it should include the assessment of the bridge performance in a critical situation with the influence of debris, log impact, scour and buoyancy of the structure. Forces due to flood can be represented by following categories.

- Forces on piers due to water flow
- Forces on superstructure due to water flow
- Forces due to debris

- Forces due to log impact
- Effects due to buoyancy

The effect of highest recorded flood of 2.32 m/s @ 111.585 m has been considered in analysis of the headstock after consultation with QDMR.

### **2.3.2 Load combinations**

In the analysis for Serviceability Limit State and Ultimate Limit State, a combination of loads should be considered and the design is to be carried out for the most critical situation.

#### **2.3.2.1 Classification of loads and load effects**

Austrroads Bridge code divides the load effects into permanent effects and transient effects

##### *2.3.2.1.1 Permanent effects*

- Structure dead load
- Superimposed dead loads
- Normal water flow and buoyancy
- Shrinkage and creep effects
- Prestressed effects (before and after losses)
- Bearing friction or stiffness forces and effects
- Differential settlement effects

##### *2.3.2.1.2 Transient effects*

- Vehicular traffic loads including dynamic effects
- Pedestrian traffic loads
- Wind loads
- Earthquake loads
- Flood loads including debris and impact loading

#### **2.3.2.2 Load combination for serviceability limit state**

In this analysis more than one transient loads can be present at any time. The basic combination is:

*Permanent Effect + (Serviceability design load for one transient or thermal effect) + k(Serviceability design load for one or more other transient or thermal effects)*

#### **2.3.2.3 Load combination for ultimate limit state**

The basic combination for this analysis is:

*Permanent effect + ultimate traffic load*

*Permanent effect +ultimate flood load*

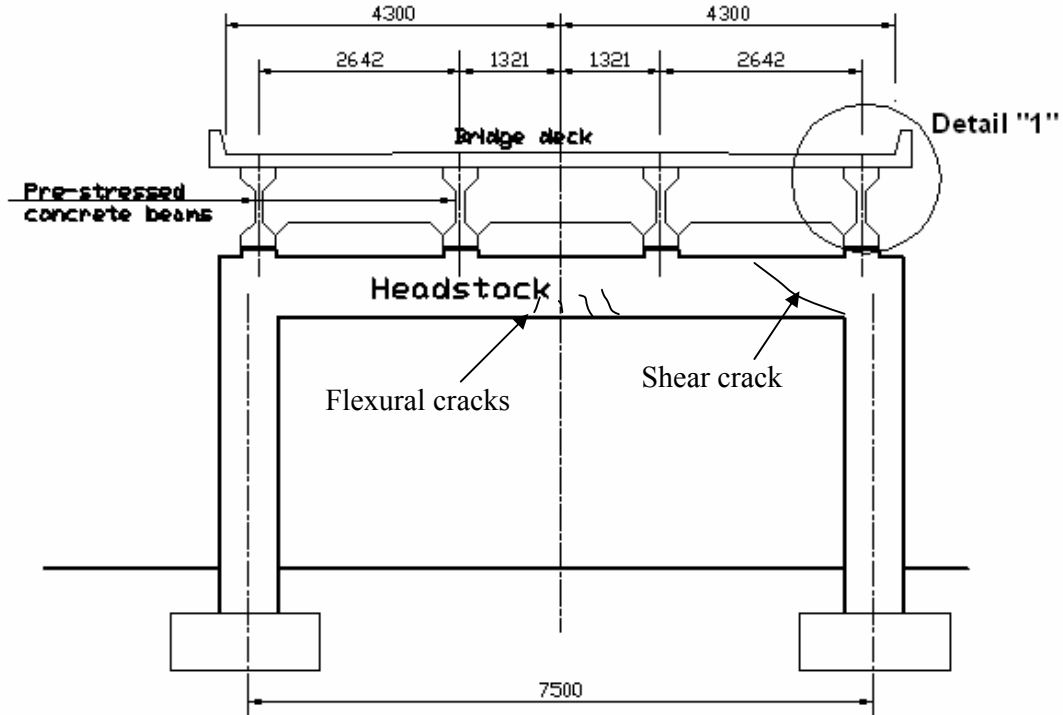
*Permanent effect + ultimate flood load + serviceability traffic loads*

*Permanent effect + ultimate traffic load + serviceability flood loads*

## 2.4 Observed damage to the headstock

The bridge has two headstocks supporting the pre-stressed concrete beams. In headstock 1, flexural cracking only is observed while headstock 2, both flexural cracking and shear cracking are observed. A photo of the damaged headstock is shown in Figure 2-5.

Figure 2-5: Observed cracks in the headstock



### **3 EVALUATION OF THE EXISTING DESIGN ACTIONS ON THE BRIDGE HEADSTOCK**

The first stage of the rehabilitation of the bridge headstock is identifying the headstock deficiencies. The deficiencies may be caused by the twin effects of deteriorating bridge infrastructure and increasing traffic loads. These combine to create the situation where the bridge is potentially unsafe.

QDMR has a comprehensive asset management system of inspections, condition data, analysis and prioritisation tools, maintenance manuals, and heavy load routing systems (Fenwick & Rotolone 2003). The asset management system aims to maintain the bridges in a condition that allows heavy vehicles free access to all parts of the network. In other words, avoid placing load restrictions on any bridge in the primary (state-controlled roads) network. The Tenthill Bridge has been observed to require immediate strengthening to avoid such restriction.

The suitable rehabilitation system for the headstock would be decided based on condition assessment of the existing structure including establishing its existing load-carrying capacities and their cause, and determining the condition of the concrete substrate. The overall evaluation should include a thorough field inspection, review of existing design or as-built documents, and a structural capacity analysis in accordance with AS 3600 and Austroads Bridge Code (1992). Existing construction and operational documents for the bridges need to be reviewed, including the design drawings, project specifications, as-built information and past repair documentation. It also needs to identify the strategic function and level of use of the route.

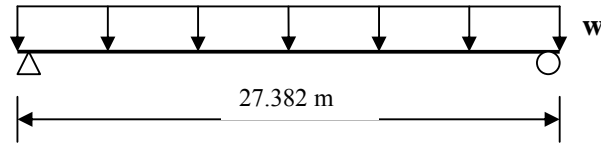
Deficient bridges can be categorized into two types as functionally obsolete and structurally deficient. Functionally obsolete bridges are the ones that cannot meet the new strategic function and level of use of the route including traffic, width, alignment, height clearance and flood frequency. Structurally deficient bridges are the one that have inadequate load carrying capacity. The Tenthill Bridge would be categorized based on the following structural capacity analysis.

#### **3.1 Structural Analysis of the Headstock**

The headstock has been analysed as a portal frame considering all necessary design situations and load combinations according to Austroad Bridge Code (1992) for ultimate limit state and serviceability limit state, which were outlined in chapter 2. The grillage analysis (lane analysis) was used to calculate traffic load on the headstock. The traffic loading models of T44 and HLP 300 in one and two lanes were used in grillage analysis. The computer program of Space Gass has been used by DMR and research team used SAP2000 computer program to check the structural analysis.

Pre-stressed beams were analyzed as simply supported beams to determine the applied dead load from the secondary beams on the headstock (see Figure 3-1).

Figure 3-1 Applied dead load on the headstock



### 3.2 Maximum design bending moments and shear

The structural analysis results from the research team are in a good agreement with the DMR analysis results. The analysis results for ultimate and serviceability stages based on DMR analysis are as follows:

Ultimate Limit State:

$$V^* = 2720 \text{ kN (2xT44 + Drag Pier Ult + Drag Super Ult + Log Ult + SW Ult)}$$

$$(M^+)^* = 4202 \text{ kN-m (2xT44 + SW Ult)}$$

$$(M^-)^* = 6244 \text{ kN-m (Drag Pier Ult + Drag Super Ult + Log Ult + SW Bouyant Ult)}$$

Serviceability Limit State:

$$V^* = 1324 \text{ kN (2xT44 + Drag Pier + Debris+ SW Ult)}$$

$$(M^+)^* = 2758 \text{ kN-m (2xT44 + SW)}$$

$$(M^-)^* = 1366 \text{ kN-m (Drag Pier + Debris + SW Bouyant Ult)}$$

Using the same model with HLP 320 heavy platform loading resulted in

$$V^* = 1797 \text{ kN (serviceability) and } 2526 \text{ kN (Ultimate)}$$

$$(M^+)^* = 3954 \text{ kN-m (serviceability) and } 5520 \text{ kN (Ultimate)}$$

The following conclusions can be drawn from the QDMR structural analysis:

- Maximum ultimate shear occurs in case of full traffic loading combined with maximum flood loads
- Maximum ultimate negative bending moment occurs in case of flood loads and floating
- Based on this analysis the cracks should not appear
- Flexural cracks may appear in heavy load platform load case

According to Austroads Bridge design code (1992) the structure should be designed for a combination of the permanent effect, the ultimate flood load and serviceability traffic loads, Hence the reported maximum negative bending moment and shear force (QDMR calculations) are not valid as the strengthening target. After consulting with QDMR, it was decided to set the strengthening target for ultimate bending moment and shear force resulted from combination of ultimate traffic loads of HLP 300 and permanent effect (dead load).



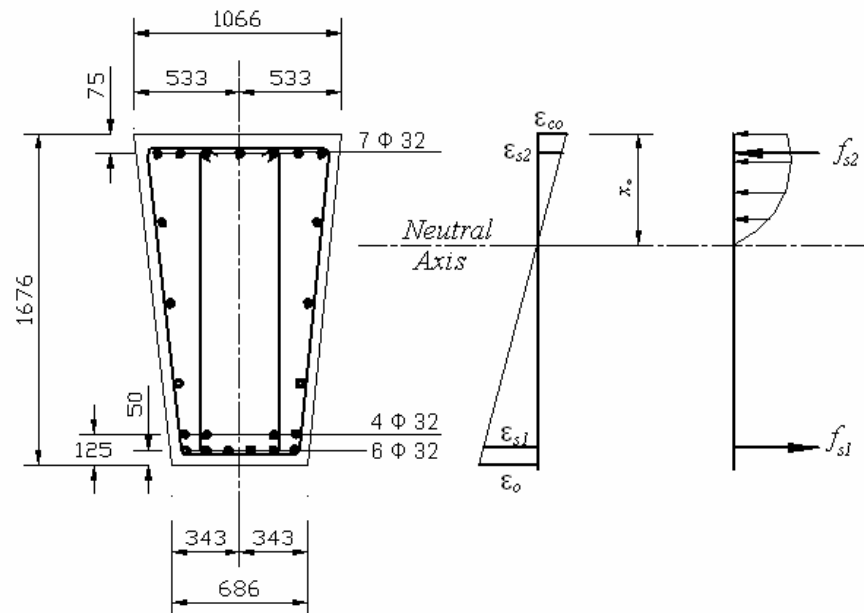
## 4 CALCULATION OF THE EXISTING CAPACITY OF THE HEADSTOCK

### 4.1 Assumptions Relating to the Capacity Analysis

In accordance with the Australian codes of practice for structural design, the capacity analysis methods contained in this section are based on ultimate limit-state philosophy. This ensures that a member will not become unfit for its intended use. The capacity analysis results would be compared with structural analysis results to identify the deficiencies. This approach sets acceptable levels of safety against the occurrence of all possible overload situations. The nominal strength of a member is assessed based on the possible failure modes and subsequent strains and stresses in each material.

A typical beam section of the headstock is shown in Figure 4-1 . The positive and negative flexural and shear capacities of the section were calculated in accordance with Australian standards (AS3600, 1988). The nominal steel –rebars areas, nominal steel yield strength of 400 MPa for longitudinal reinforcement and 240 MPa for shear reinforcement and nominal concrete compressive strength of 20 MPa were used in the section capacity analysis. The degradation due to corrosion of the steel and creep and shrinkage of the concrete were ignored.

Figure 4-1: Beam section of headstock and internal strain stress distribution



### 4.2 Residual Flexural Capacity of the Headstock

The following assumptions form the basis for the calculation of the ultimate strength of the concrete element strengthened in flexure.

- Design calculations are based on the actual dimensions, internal reinforcing steel arrangement, and material properties of the existing member.
- The strain in reinforcement and concrete are directly proportional to the distance from the neutral axis, that is, a plane section before loading remains plane after loading.

The residual capacity of the bridge headstock is calculated in accordance with Austroads clause 5.8.1.2 and 5.8.1.3.

$$f'_c = 21 \text{ MPa}, f_{sy} = 400 \text{ MPa}$$

$$M_u = f_{sy} A_{st} d \left( 1 - 0.6 \frac{A_{st} f_{sy}}{bd f'_c} \right)$$

$$M_u = 400 \times 8030 \times 1600 \left( 1 - 0.6 \frac{8030}{1600 \times 876} \times \frac{400}{21} \right) = 4800 \text{ kN-m}$$

$$\phi M_u = 0.8 \times 4800 = 3840 \text{ kN-m ( In agreement with DMR calculations)}$$

### 4.3 Residual capacity of the bridge headstock in shear

Shear strength of the beam is calculated in accordance with Austroads Bridge code clause 5.8.2.

$$\phi V_u = \phi (V_{uc} + V_{us})$$

$$V_{uc} = \beta_1 \beta_2 \beta_3 bd \left( \frac{A_{st} f'_c}{bd} \right)^{1/3} \quad (\text{Austroads Bridge code 5.8.2.7})$$

$$\beta_1 = \left( 1.4 - \frac{1620}{2000} \right) = 0.59 \geq 1.1$$

$$\beta_3 = (2d/a_v) = \left( 2 \times 1620 / 1680 \right) = 1.92$$

$$V_{uc} = 1.1 \times 1.0 \times 1.92 \times 876 \times 1620 \left( \frac{8030 \times 21}{876 \times 1620} \right)^{1/3} = 1475 \text{ kN}$$

*(Different from DMR analysis due to use of different factors of  $\beta_1$  and  $\beta_3$ )*

$$V_{us} = \frac{A_{sv} f_{sv} d}{s} \cot \theta_v = \frac{804 \times 230 \times 1676}{250} \times 1 = 1475 \text{ kN (In agreement with DMR calculations)}$$

$$\phi V_u = 0.7 \times 2950 = 2065 \text{ kN}$$

$$V^* = 2720 \text{ kN} > \phi V_u = 2065 \text{ kN} \text{ need strengthening (RMIT)}$$

$$\phi V_u = 1537 \text{ kN} \text{ need strengthening ( DMR)}$$

$$M^* = 5520 \text{ kN-m} > \phi M_u = 3840 \text{ kN} \text{ need strengthening}$$

The above calculations are based on uncracked strength of the reinforced concrete beam. Design codes do not provide any guidelines on calculation of the shear strength of a reinforced concrete beam with a diagonal crack. This area requires further research. A literature review indicated that 15 to 20% reduction in capacity can be expected in a beam with a diagonal crack compared to uncracked shear strength.

## 5 STRENGTHENING OF THE BRIDGE HEADSTOCK WITH EXTERNAL POST-TENSIONING

Pre-stressed concrete is composed of concrete, high strength steel tendons and normal reinforcing steel. In the construction process, tendons are tensioned against hardened concrete. This hardened concrete is in a state of permanent precompression. In post-tensioning the tendons are stressed after the concrete has hardened to carry the expected loads. Post-tensioning is used to increase the capacity of the headstock.

### 5.1 Design parameters

For post-tensioning strengthening of the bridge headstock, wire strands or bars can be used as the pre-stressing tendons. In this particular case study, it was decided to use steel bar of diameter 38 mm. The minimum breaking load and tensile strength of the bars are 1230 kN and 1080 MPa respectively. The yield strength of bars would be  $0.85 f_p$  where  $f_p$  is the minimum tensile strength (Clause 6.3.1 of AS 3600). Therefore it is 918 MPa. Total area of prestressing steel is  $4 \times 1140 = 4560 \text{ mm}^2$ . (QDMR calculations)

### 5.2 Structural calculations

It is assumed that the strengthening is in accordance with the current calculations of post-tensioning method. Based on the preliminary calculations it was decided to use 4 bars of 38 mm diameter as the pre-stressing steel. From Table 6.3.1 of Australian Standards (AS 3600), the minimum breaking load for this particular steel bar should be 1230 kN. However in the DMR calculations, the breaking load is being taken as 1225 kN.

$$I = 2.691 \times 10^{11} \text{ mm}^4 \quad Q = 241 \times 10^6 \text{ mm}^3 \quad A = 686 \times 1676 = 1.15 \times 10^6 \text{ mm}^2 \\ V^* = 2720 \text{ kN}, \quad M^* = 5520 \text{ kN-m}$$

With 20% reduction in the breaking force, the prestressing force for one bar is calculated as 980 kN. Therefore the total prestressing force is obtained as,

$$P = 4 \times 980 = 3920 \text{ kN (QDMR calculations)}$$

Using this pre-stressing force, the shear and flexural capacities of the pre-stressed beam would be presented in the following sections.

#### 5.2.1 Shear capacity

Pre-stressing has a significant influence in the load capacity in shear and shear in diagonal cracking of a pre-stressed member. The flexural and inclined crack formation can be delayed with the horizontal component of pre-stressing force. The vertical component of the pre-stressing force affects the shear force acting on concrete. Shear capacity after post-tensioning strengthening needs to be checked for the loads at both flexural-shear cracking and web shear cracking.

##### 5.2.1.1 Flexural-shear cracking

The ultimate shear strength of a pre-stressed beam is given below in accordance with the Clause 5.8.2.7 of Austroads Bridge code.

$$V_{uc} = \beta_1 \beta_2 \beta_3 \beta_v d_0 \left( \frac{A_{st} f'_c}{b_v d_0} \right)^{1/3} + V_0 + P_v$$

The first component of  $V_{uc}$  is the same as given in Section 4.3,  $V_o$  is the shear force at the section when the bending moment is equal to decompression moment ( $M_o$ ) and  $P_v$  is the vertical component of the pre-stressing force.

In this particular case study, we can use the first component of  $V_{uc}$  from Section 4.3 and there is no vertical component of the pre-stressing force. Therefore if the decompression moment for the section of the beam,  $M_o$  is known, the ultimate shear strength of beam can be calculated. The decompression moment  $M_o$  is,

$$M_o = Z_b (P_e/A) = 3.21 \times 10^8 (3920/1676 \times 686) = 1095 \text{ kN-m}$$

$$V_o = \frac{M_o}{(M^*/V^*)}$$

Therefore  $V_o = 1095 \times 2720 / 5520 = 539 \text{ kN}$  and finally,

$$\phi V_u = 1537 + 0.7 \times 539 = 1914 \text{ kN (DMR)} < V^* = 2720 \text{ kN}$$

$$\phi V_u = 2065 + 0.7 \times 539 = 2442 \text{ kN (RMIT)} < V^* = 2720 \text{ kN}$$

### 5.2.1.2 Web shear cracking

The web shear cracking load can be obtained by equating the tensile strength of concrete to the principal tensile stress at a critical point in the web.

$$V_{uc} = V_t + P_v \quad (\text{Austroads Bridge code 5.8.2.7})$$

$V_t$  is the shear force at the principal tensile cracking and  $P_v$  is the vertical component of the pre-stressing force. In this case study, there is no vertical component of the pre-stressing force.

The direct stress due to pre-stressing is,

$$\sigma = -P/A = -3.41 \text{ MPa}$$

The shear stress is,

$$\tau = \frac{V_t Q}{Ib} = 1.305 \times 10^{-6} V_t \text{ MPa}$$

it is assumed that principal tensile stress of  $\sigma_1 = 0.33\sqrt{f'_c}$  will cause diagonal cracking.

Therefore

$$\sigma_1 = 0.33\sqrt{f'_c} = 0.33\sqrt{20} = 1.476 \text{ Mpa}$$

is sufficient to cause a diagonal crack. Using Mohr circle,

$$\sigma_1 = \sqrt{\left(\frac{\sigma}{2}\right)^2 + \tau^2} + \frac{\sigma}{2} = \sqrt{\left(\frac{-3.41}{2}\right)^2 + \tau^2} + \frac{-3.41}{2} = 1.476$$

Therefore  $V_t = 2057 \text{ kN}$

Shear at web shear cracking is therefore,

$$V_{uc} = V_t$$

$$\phi V_u = 0.7 (V_{us} + V_{uc}) = 0.7 (V_{us} + V_t) = 0.7 (1475 + 2057) = 2472 < V^* = 2720 \text{ kN}$$

A question is raised about sliding failure of the beam along the shear crack at high pre-stress forces. Therefore post tensioning solution perhaps requires an upper limit imposed on the applied pre-stress force to prevent this. A search of literature did not yield any published work covering this area. A simple friction calculation can be done to establish an approximate upper limit.

### 5.2.2 Flexural capacity

In pre-stressed concrete beams, pre-stressing steel is tensioned during the construction. This results in a pre-compression force in concrete. In the post cracking behaviour, the pre-stressing steel in the tensile region causes a significant contribution to the moment capacity of the section.

Approximate calculation for  $M_u$  with pre-stressing steel and reinforcing steel would be,

$$M_u = f_{sy} A_{st} (d - \alpha d) + F_{py} (d_p - \alpha d)$$

$\alpha$  is an assumed value for the depth of the line of action of the resultant compressive force (concrete and steel). A reasonable approximation would be  $0.15 d_{st}$ . Therefore,

$$M_u = 400 \times 8030 \times 1600 (1 - 0.15) + 980000 \times 4 (1126 - 0.15 \times 1600) = 7841 \text{ kNm}$$

$$\phi M_u = 0.8 \times 7841 = 6273 \text{ kNm}$$

## **6 STRENGTHENING OF THE BRIDGE HEADSTOCK USING FRP COMPOSITES**

### **6.1 Background**

Initial discussion with the structures division of QDMR has indicated that there are some specific concerns which inhibited ready acceptance of FRP composites for regular strengthening schemes. These stem from concerns about the lack of design guidelines in accordance with the Austroads code (1992), brittleness of the failure mode of FRP wrapping schemes by FRP fracture as well as de-bonding, lack of information on durability and fire-resistance and difficulty in selecting a product to suit a given application without completely relying on the supplier of FRP products. In addressing these issues, the research team has reviewed all the published research on the topic and established the state-of-the art. Subsequently they developed a procedure for applying these outcomes systematically to the practical strengthening project, which is reported herein.

### **6.2 Design Guidelines**

Since the use of FRP composites for strengthening of reinforced concrete structures is a relatively new technique, the development of design guidelines for externally bonded FRP system is ongoing in Europe, Japan, Canada and the United States. Within the last ten years, many design guidelines have been published to provide guidance for the selection, design and installation of FRP systems for externally strengthening of concrete structures. In Europe, Task Group 9.3 of the international Federation for Structural Concrete published bulletin 14 (FIB 14) on design guidelines for externally bonded FRP reinforcement for reinforced concrete structures. And in the United States, ACI Committee 440 developed a guide for the design and construction of externally bonded systems for strengthening concrete structures. Applications of provisions of these two guidelines are fully covered here.

### **6.3 Design of FRP System**

In accordance with the Australian codes of practice for structural design, the design methods contained in this report are based on limit-state design philosophy. This ensures that a strengthened member will not become unfit for its intended use. It will not also fail at an accidental overload during its design life with 95% confidence. All necessary design situations and load combinations would be considered, which were outlined in Chapter 2. In assessing the effect of a particular limit state on the structure, it is required to assume certain values for the design loading and the design strength of the materials. The design load factors were also outlined in Chapter 2 and design material properties will be discussed in this chapter. This approach sets acceptable levels of safety against the occurrence of all possible failure modes.

The nominal strength of a member is assessed based on the possible failure modes and subsequent strains and stresses in each material. The design of the FRP composites involves assessing the effects of the additional FRP reinforcement provided to the section (designed assuming full composite action) and the ability of transferring forces by means of the bond interface. All possible failure modes should be investigated for a FRP strengthened section (Ganga Rao and Vijay 1998). In general, the failure modes can be subdivided to those assuming full composite action between the reinforced concrete / pre-stressed

concrete member and the FRP and those verifying the different de-bonding mechanisms that may occur. The state of the structure prior to strengthening is taken as a reference for the design of the externally bonded FRP reinforcement. The strength of strengthened member depends on the controlling failure mode.

It was decided to bond FRP laminates to the tension face of the beam section (bottom fibre) of the headstock with fibres oriented along the length of the member for positive flexural strengthening and use a complete wrapping scheme with fibres oriented along the transverse axis of the beam section for the shear strengthening. It was decided to use Sika CFRP laminate CarboDur type S for flexural strengthening and Sika CFRP wet lay up type Sika-Wrap-230C . Table 6-1 shows material properties of proposed systems.

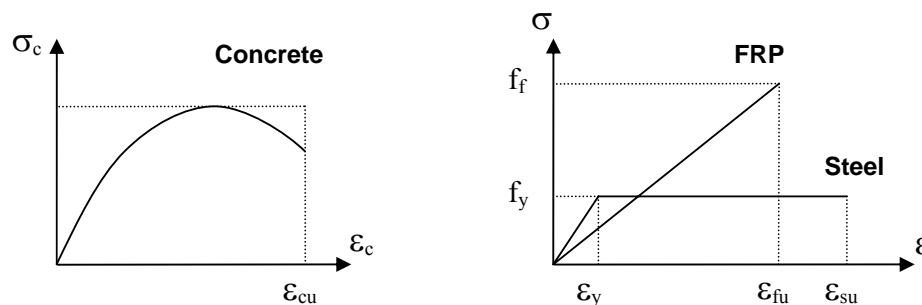
Table 6-1 Material properties of FRP systems

TYPE	Tensile Strength (MPa)	Tensile Elastic Modulus (MPa)	Elongation at Break
CarboDur Type S	2800	165000	1.7%
Sika-Wrap-230C	3500	230000	1.5%

## 6.4 Flexural Strengthening

In the analysis for the ultimate state in flexure, both codes follow well established procedures using idealised stress-strain curves for concrete, FRP and longitudinal reinforcement.

Figure 6-1 Idealised stress-strain curves for constitutive materials at ULS



These curves, along with the following assumptions, form the basis for the ultimate strength ultimate state analysis of a concrete element strengthened in flexure.

- Design calculations are based on the actual dimensions, internal reinforcing steel arrangement, and material properties of the existing member being strengthened.
- The strain in reinforcement and concrete are directly proportional to the distance from the neutral axis, that is, a plane section before loading remains plane after loading.
- There is no relative slip between external FRP reinforcement and the concrete
- The shear deformation within the adhesive layer can be neglected since the adhesive layer is very thin with slight variations in its thickness.

The cross section analysis identifies all possible failure modes. Failure of the strengthened element may then occur as a result of various mechanisms as follows:

- Crushing of the concrete in compression before yielding of the reinforcing steel
- Yielding of the steel in tension followed by rupture of the FRP laminates
- Yielding of the steel in tension followed by concrete crushing
- Shear/tension de-lamination of the concrete cover
- De-bonding of the FRP from the concrete substrate

#### 6.4.1 Design material properties

According to the FIB guideline, the design strength is obtained by dividing the characteristic strength by a partial safety factor. The partial safety factors for concrete (in flexure),  $\gamma_{mc}$ , and steel reinforcement,  $\gamma_{ms}$ , are normally taken as 1.5 and 1.15 respectively. The partial safety factors applied on characteristic strength of FRPs are mainly based on the observed differences in the long-term behaviour of FRP (basically depending on the type of fibres) as well as the application method and on-site working conditions. A partial safety factor for carbon fibre in application type B under difficult on-site working condition,  $\gamma_{ms}$ , of 1.35 is indicated. The design material properties for the headstock according to the FIB guideline are listed in *Table 6-2*.

*Table 6-2 Design material properties complying with the FIB guideline*

Material	Design Strength (MPa)	Modulus of Elasticity (MPa)	Allowable strain
Concrete	21/1.5=14	22610*	0.0035
Steel reinforcement	400/1.15=348	200000	0.002
CFRP strips (flexural)	2800/1.35=2047	165000	0.017/1.35=0.0126
CFRP wrapping (shear)	3500/1.35=2593	230000	0.015/1.35=0.0111

\*The long term modulus of elasticity of 11305 was used to account for creep of concrete

ACI design guideline suggests that the design ultimate tensile strength should be determined using the environmental reduction factor only for FRP materials. The reduction factors are mainly based on type of fibre and environmental conditions. Similarly it is suggested to reduce the design rupture strain for environmental-exposure conditions. A reduction factor for carbon fibre in aggressive environment,  $C_E$ , of 0.85 is indicated. The design material properties for the headstock according to the ACI guideline are listed in *Table 6-3*.

*Table 6-3 Design material properties according to the ACI guideline*

Material	Design Strength (MPa)	Modulus of Elasticity (MPa)	Allowable strain
Concrete	21 ( $\beta_1=0.91$ )	22610*	0.003
Steel reinforcement	400	200000	0.002
CFRP strips (flexural)	0.85x2800=2380	165000	0.85x0.017=0.01445
CFRP wrapping (shear)	0.85x3500=2975	230000	0.85x0.015=0.01275

\*The long term modulus of elasticity of 11305 was used to account for creep of concrete

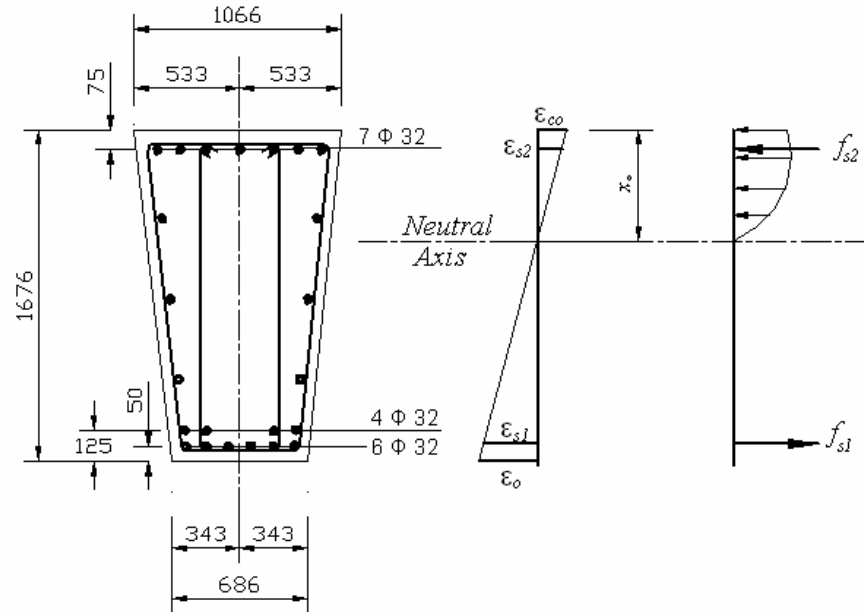
#### 6.4.2 Initial situation

It was noted by both design guidelines that the effect of the initial load prior to strengthening should be considered in the calculations using the theory of elasticity and with the service moment acting on the critical beam section during strengthening. The initial strain distribution



of the member may then be evaluated and considered in strengthening calculations. As the service bending moment is typically greater than the cracking moment, the calculation is based on a cracked section. The initial strain distribution of the headstock was calculated based on structural analysis for service loading condition, long-term modulus of elasticity and the cracked section. The same initial strain distribution was used in calculation of the capacity of the strengthened member using both design guidelines.

Figure 6-2 Initial situation



$$x_o = 777 \text{ mm} \Rightarrow \varepsilon_{co} = \frac{M_o x_o}{E_c I_{co}} = \frac{2758 \times 10^6 \times 777}{22610 \times I_{co}}$$

$$I_{co} = 1.6 \times 10^{11} + (10 - 1) \times 5521 \times (777 - 75)^2 + 10 \times 8030 \times 823^2 = 2.39 \times 10^{11}$$

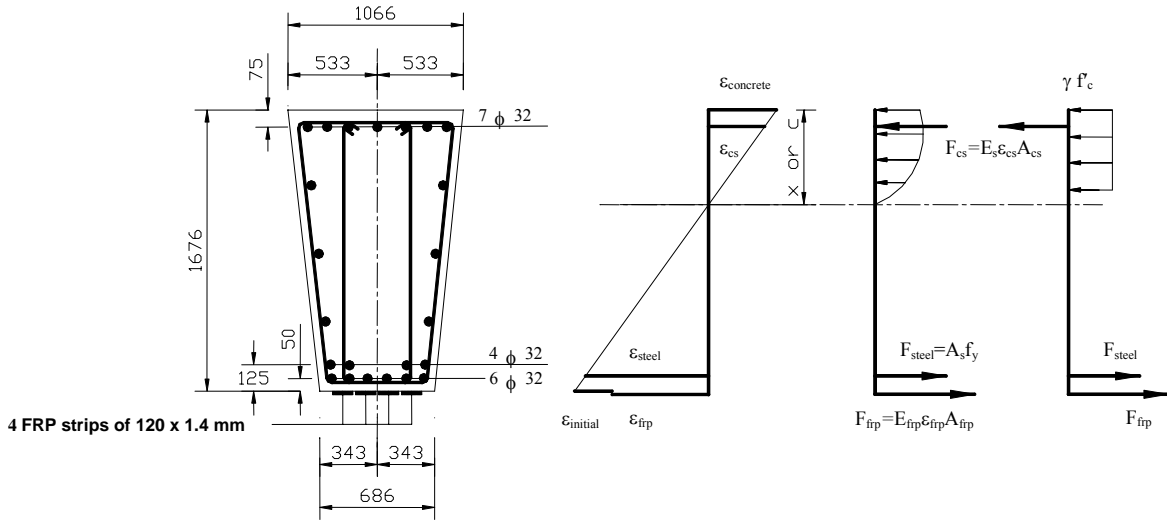
$$\Rightarrow \varepsilon_{co} = \frac{M_o x_o}{E_c I_{co}} = \frac{2758 \times 10^6 \times 777}{22610 \times I_{co}} = 0.0004$$

$$\Rightarrow \varepsilon_o = \varepsilon_{co} \frac{h - x_o}{x_o} = 0.0004 \times \frac{1676 - 777}{777} = 0.00046$$

### 6.4.3 Capacity of the strengthened beam

The cross section analysis indicated that the failure mode of the beam section of the headstock would be the yielding of the longitudinal steel reinforcement followed by concrete crushing, while the FRP is intact. This is the most desirable failure mode, which satisfy the safety requirements in ultimate state for a reinforced concrete section. The design bending moment for the strengthened member was then calculated in accordance with each design guidelines based on well established principles of flexural design of a reinforced concrete beam. The design principals are shown in Figure 6-3.

Figure 6-3 Internal strain and stress distributions for the beam cross section of the headstock



The section design for failure mode of yielding steel followed by concrete crushing

Flexural strengthening based on FIB14:

Calculation of neutral axis depth,  $x$ :

$$0.85\psi f'_{cd} bx + A_{s2} E_s \varepsilon_{s2} = A_{s1} f_{yd} + A_f E_f \varepsilon_f$$

Try use of 4 FRP strips of 120 x 1.4

$$0.85 \times 0.8 \times \frac{21}{1.5} \times 980x + 5621 \times 200000 \varepsilon_{s2} = 8030 \times \frac{400}{1.15} + 672 \times 165000 \varepsilon_f$$

$$\varepsilon_f = \varepsilon_{cu} \frac{h-x}{x} - \varepsilon_o$$

$$\varepsilon_{s2} = \varepsilon_{cu} \frac{x-d_2}{x} - \varepsilon_o$$

$$x = 312 \text{ mm}, \quad \varepsilon_f = 0.0138 < 0.017 \quad \varepsilon_{s2} = 0.0012$$

$$M_{RD} = A_{s2} E_s \varepsilon_{s2} (\delta_G x - d_2) + A_{s1} f_{yd} (d - \delta_G x) + A_f E_{fu} \varepsilon_f (h - \delta_G x)$$

$$M_{RD} = 5621 \times 200000 \times 0.0012 (0.4 \times 312 - 75) + 8030 \frac{400}{1.15} (1660 - 0.4 \times 312) + 672 \times 165000 \times 0.0138 \times (1676 - 0.4 \times 312) = 6729 \text{ kN} \cdot \text{m}$$

Flexural strengthening based on ACI440:

$$f'_c = 21$$

$$\beta_1 = 1.09 - 0.008f'_c = 0.92 \quad (\text{ACI 318-99, Section 10.2.7.3})$$

$$E_c = 57000\sqrt{f'_c} = 261000$$

$$\rho_{s1} \equiv \frac{A_s}{bd} = \frac{8030}{1676 * 876} = 0.0055$$

$$\rho_{s2} \equiv \frac{A_s}{bd} = \frac{5521}{1676 * 876} = 0.0038$$

$$\rho_f \equiv \frac{A_f}{bd} = \frac{672}{1676 * 876} = 0.00045$$

$$nE_f t_f = 165000 \times 1.4 = 231000 > 180000$$

$$\kappa_m = \frac{1}{60\varepsilon_{fu}} \left( \frac{90000}{nE_f t_f} \right) = \frac{1}{60 \times 0.01445} \left( \frac{90000}{231000} \right) = 0.45 < 0.9 \quad (\text{ACI 9-2})$$

$$\varepsilon_f = \varepsilon_{cu} \frac{h-x}{x} - \varepsilon_o$$

$$\varepsilon_{s2} = \varepsilon_{cu} \frac{x-d_2}{x} - \varepsilon_o$$

$$x = \frac{A_{s1}f_{sy} + A_f E_f \varepsilon_f - A_{s2} E_s \varepsilon_{s2}}{f'_c \beta_1 b}$$

$$x = 244 \text{ mm}, \quad \varepsilon_f = 0.01146 < 0.01445 \quad \varepsilon_{s2} = 0.00087$$

$$\phi M_n = 0.9 \left[ A_{s2} E_s \varepsilon_{s2} \left( \frac{\beta_1 x}{2} - d_2 \right) + A_{s1} f_{sy} \left( d - \frac{\beta_1 x}{2} \right) + \psi A_f E_f \varepsilon_f \left( h - \frac{\beta_1 x}{2} \right) \right]$$

$$\phi M_n = 0.9 \left[ \frac{5621 \times 200000 \times 0.00087 (111 - 75) + 8030 \times 400 (1600 - 111) + 0.85 \times 672 \times 165000 \times 0.01146 \times (1676 - 111)}{1} \right] = 5854 \text{ kN-m}$$

The design bending moment capacity was then calculated based on each of the design guidelines. The design bending moment capacity of 6720 kN-m and 5854kN-m were calculated for strengthened section based on the FIB and ACI design guidelines respectively. Although both the design guidelines use the same principal to calculate the capacity of the strengthened member, each design guideline introduces different values for ultimate strain of the concrete and the strength reduction and material safety factors. The calculated moment capacities using the two design guidelines indicated that the predicted capacity enhancement based on the ACI guideline is more conservative. This is mainly due to the use of the strength reduction factors ( $\phi$ ) required by ACI 318-99 with an additional strength reduction factor of 0.85 applied to the contribution of FRP reinforcement to flexural capacity enhancement.

#### 6.4.4 Anchorage

Experimental investigations show that the FRP rupture is a rare event and delamination of FRP strips is more likely occur before stress in the FRP reach the ultimate level. Debonding implies the complete loss of composite action between the concrete and FRP laminates. Bond failure will be a brittle failure and should be prevented at any cost. The ACI guideline place a limitation on the strain level in the laminate to prevent delamination of FRP from the concrete substrate.

$$nE_f t_f = 165000 \times 1.4 = 231000 > 180000$$

$$\kappa_m = \frac{1}{60\varepsilon_{fu}} \left( \frac{90000}{nE_f t_f} \right) = \frac{1}{60 \times 0.01445} \left( \frac{90000}{231000} \right) = 0.45 < 0.9 \quad (\text{ACI 440 9-2})$$

$$\varepsilon_f = \varepsilon_{cu} \frac{h-x}{x} - \varepsilon_o \leq \kappa_m \varepsilon_{fu} = 0.45 \times 0.01445 = 0.0065 \quad (\text{ACI 440 9-3})$$

$$T = E_f \varepsilon_{fe} A_f = 165000 \times 0.0065 \times 672 = 720000 N$$

$$T = \frac{M \alpha_f A_f (h-x)}{I_{cs}}$$

$$720,000 = \frac{M \times 14.53 \times 672(1676 - 513)}{2.63 \times 10^{11}} \Rightarrow M = 16698 kN - m > M_n$$

The FIB guideline noted that the following failure modes need to be considered to prevent de-lamination of FRP, depending on the starting point of the de-bonding process.

- De-bonding in an un-cracked anchorage zone
- De-bonding caused at flexural cracks
- De-bonding caused at shear cracks

De-bonding of CFRP strips was checked based on each guideline and the calculations (given below) indicated that the strengthening system satisfies the requirements from both guidelines to prevent the de-bonding failure. It seems that the FIB guideline uses a more accurate methodology to check the de-bonding failure which considers all possible failure modes. However the de-bonding failure of CFRP strips in the strengthening of the headstock will be also controlled by applying CFRP wrapping scheme applied for shear strengthening.

*Approach 1: Verification of end anchorage, Strain limitation in the FRP,*

This approach involves two independent steps: first, the end anchorage should be verified based on the shear stress-slip constitutive law at the FRP-concrete interface. Then strain limitation should be applied on the FRP to ensure that bond failure far from the anchorage is

prevented. In the following the model of Holzenkamper (1994) as modified by Neubauer and Rostasy (1997) is presented

$$N_{fa,max} = \alpha c_1 k_c k_b b \sqrt{E_f t_f f_{ctm}} \quad (\text{N}) \quad (\text{FIB A1-1})$$

$$l_{b,max} = \sqrt{\frac{E_f t_f}{c_2 f_{ctm}}} \quad (\text{mm}) \quad (\text{FIB A1-2})$$

$$l_{b,max} = \sqrt{\frac{165000 \times 1.4}{2 \times 2}} = 240 \text{mm}$$

$$k_b = 1.06 \sqrt{\frac{2 - \frac{b_f}{b}}{1 + \frac{b_f}{400}}} = 1.06 \sqrt{\frac{2 - \frac{480}{686}}{1 + \frac{480}{400}}} = 0.81 < 1 \quad (\text{FIB A1-3})$$

$$N_{fa,max} = \alpha c_1 k_c k_b b_f \sqrt{E_f t_f f_{ctm}} = 0.9 \times 0.64 \times 1.0 \times 1.0 \times 480 \sqrt{165000 \times 1.4 \times 2} = 188 \text{kN}$$

Theoretical cut off point

$$N_{fa,max} = \frac{M \alpha_f A_f (h - x)}{I_{cs}}$$

$$188,000 = \frac{M \times 14.53 \times 672(1676 - 513)}{2.63 \times 10^{11}} \Rightarrow M = 4354 \text{kN} - \text{m}$$

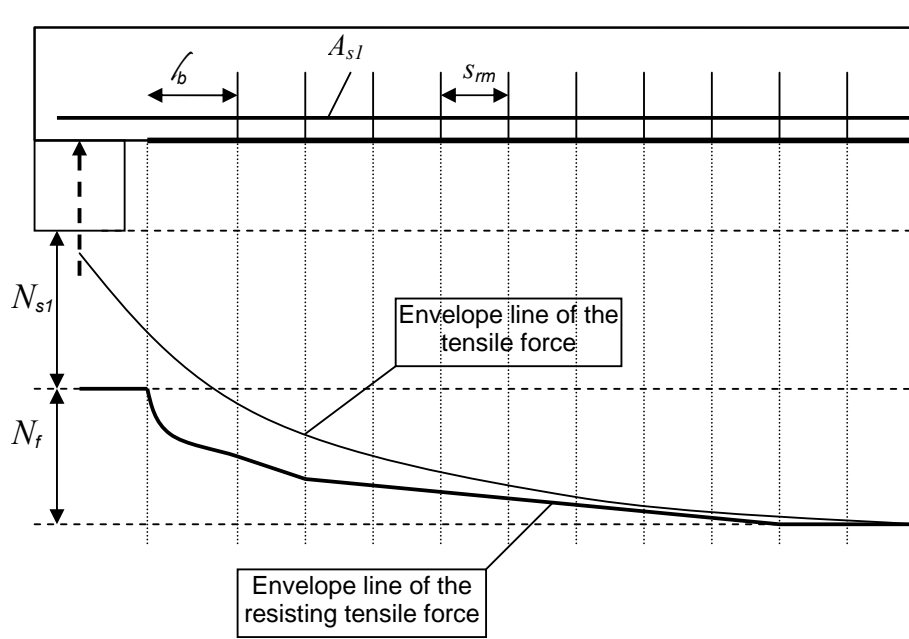
Based on structural analysis (Load combination of ultimate HLP 300 and ultimate dead load), the bending moment of 4300 kN-M occur at 0.45 m from the beam support middle span towards the column. Hence the anchorage length is 1.2 m

Provided anchorage length = 1200 mm >  $l_{b,max} = 240 \text{mm}$  (required)

*Approach2: Calculation of the envelop line of tensile stress*

A more detailed approach to prevent peeling-off at flexural cracks in case of short-term static loading is proposed by Niedermeier (2000). The aim of this approach is to calculate the maximum possible increase in tensile stress within the FRP strips, which can be transferred by means of bond stresses between two subsequent flexural cracks. This increase should be compared to the increase according to the design assumption of the full composite action.

Figure 6-4 Envelope line of the tensile forces



The basic approach consists of three steps

- Determination of the most unfavorable spacing of flexural cracks
- Determination of the tensile force within FRP strip between two subsequent cracks according to the design in bending
- Determination of the maximum possible increase in tensile stress in the FRP

Determination of the most unfavorable spacing of flexural cracks,

$$\tau_{sm} = 1.85 f_{ctm} = 1.85 \times 2 = 3.70 \quad (\text{FIB A2-1})$$

$$\tau_{fm} = 0.44 f_{ctm} = 0.44 \times 2 = 0.88 \quad (\text{FIB A2-2})$$

$$s_{sm} = 2\ell_t = 2 \frac{M_{cr}}{z_m} \frac{1}{(\sum \tau_{sm} b_f + \sum \tau_{sm} d_s \pi)} = 478 \text{mm} \quad (\text{FIB A2-3})$$

$$\max \Delta \sigma_{fd} = \frac{c_1}{\gamma_c} \sqrt{\frac{E_f \sqrt{f_{ck} f_{ctm}}}{t_f}} = \frac{0.23}{1.5} \sqrt{\frac{165000 \sqrt{21 \times 2}}{1.4}} = 134 \text{MPa} \quad (\text{FIB A2-6})$$

$$\ell_{b,\max} = c_2 \sqrt{\frac{E_f t_f}{\sqrt{f_{ck} f_{ctm}}}} = 1.44 \sqrt{\frac{165000 \times 1.4}{\sqrt{21 \times 2}}} = 210 \text{mm}. \quad (\text{FIB A2-7})$$

$$\max \Delta \sigma_{fd} = 134 \text{MPa} > \Delta \sigma_{fd} = 105 \text{MPa}$$

**Approach 3: Verification of anchorage and the force transfer between FRP and concrete**

The verification of the end anchorage has already been performed. It should be then verified that the resulted shear stress  $\tau_b$  from the change of tensile force along the FRP at the FRP-concrete interface is limited.

$$f_{cbd} = 1.8 \frac{f_{ctk}}{\gamma_c} = 1.8 \frac{2}{1.5} = 2.4 \text{MPa} \quad (\text{FIB A3-2})$$

$$\varepsilon_{s1} < \varepsilon_{yd} : \quad \frac{V_d}{0.95db_f \left( 1 + \frac{A_{s1}E_s}{A_fE_f} \right)} = 0.17 < f_{cbd} \quad (\text{FIB A3-4a})$$

$$\varepsilon_{s1} \geq \varepsilon_{yd} : \quad \frac{V_d}{\frac{z_s + z_f}{2} b_f} = 2.66 > f_{cbd} \quad (\text{FIB A3-4b})$$

Due to the substantial width of the bond interface available, the above verification is not critical. It can be seen that bond problems may occur in case of yielding of the internal reinforcement, which is in line with the safety concept. However, this requirement can be satisfied by using five strips of FRP.

De-bonding of CFRP strips was checked based on each guideline and the calculations indicated that the strengthening system satisfies the requirements from both guidelines to prevent the de-bonding failure. It seems that the FIB guideline uses a more accurate methodology to check the de-bonding failure which considers all possible failure modes. However the de-bonding failure of CFRP strips in the strengthening of the headstock will be also be controlled by CFRP wrapping scheme applied for shear strengthening.

## 6.5 Shear strengthening

The design for shear strengthening of a reinforced concrete member in both the guidelines is based on truss model and superposition principle with some considerations for the orthotropic behaviour of the CFRP material. The shear strength of a strengthened member is determined by adding the contribution of the CFRP reinforcing to the contributions from the concrete and shear reinforcement

$$V_{total} = V_{concrete} + V_{Steel} + V_{frp}$$

where  $V_{concrete}$ ,  $V_{Steel}$  and  $V_{frp}$  are the contributions from the concrete, steel and the FRP respectively.

According the ACI guideline the shear strength should be calculated using the strength-reduction factor,  $\phi$ , required by ACI 318-99.

$$\phi V_n = V_u \quad (\text{ACI 440 10-1})$$

The nominal shear strength of an FRP-strengthened concrete member can be determined by adding the contribution of the FRP reinforcement to the contributions from the shear steel reinforcement and the concrete. It is also suggested that an additional reduction factor of  $\psi_f=0.95$ , to be applied to the shear contribution of the FRP reinforcement.

$$\phi V_n = \phi(V_{uc} + V_{us} + \psi_f V_f) \quad (\text{ACI 440, 10-2})$$

$$\varepsilon_{fe} = 0.004 \leq 0.75 \varepsilon_{fu} \quad (\text{ACI 440, 10-6a})$$

$$\varepsilon_{fe} = 0.004 < 0.75 \times 0.01275 = 0.009$$

$$f_{fe} = \varepsilon_{fe} E_f = 0.004 \times 230000 = 920 \text{ MPa} \quad (\text{ACI 440, 10-5})$$

$$A_{fv} = 2n t_f w_f = 2 \times 1 \times 0.13 \times 1676 = 436 \text{ mm}^2 \quad (\text{ACI 440, 10-4})$$

$$V_f = \frac{A_{fv} f_{fe} (\sin \alpha + \cos \alpha) d_f}{S_f} = 436 \times 920 (1) = 400 \text{ kN} \quad (\text{ACI 440, 10-3})$$

$$\phi V_n = \phi(V_c + V_s + \psi_f V_f) = 0.85(1475 + 1475 + 0.95 \times 400) = 2796 \text{ kN} \quad (\text{ACI 440, 10-2})$$

$$\phi V_n = 2796 \text{ kN} > V^* = 2720 \text{ kN} \quad (\text{ACI 440, 10-1})$$

The FIB guideline uses the model of Triantafillou (1998) and Täljsten (1999 a and 1999b), the external FRP reinforcement may then be treated in analogy to the internal steel (accepting that the FRP carries only normal stresses in the principal FRP material direction), assuming that at the ultimate limit state in shear (concrete diagonal tension) the FRP develops an effective strain in the principal material direction. The effective strain is, in general, less than the tensile failure strain,  $f_u$ . Hence, the shear capacity of a strengthened element may be calculated according to the EC2 format as follows:

$$V_{Rd} = \min(V_{uc} + V_{us} + V_f, V_{Rd2}) \quad (\text{FIB5-1})$$

The FRP contribution to shear capacity,  $V_{fd}$ , can be written in the following form:

$$V_f = 0.9 \varepsilon_{fd,e} E_f \rho_f b_w d (\cot \theta + \cot \alpha) \sin \alpha = 310 \text{ kN} \quad (\text{FIB5-2})$$

$$\rho_f = 2 t_f \sin \alpha / b_w = 2 \times 0.13 (1) / 876 = 0.0003$$

$$\varepsilon_{f,e} = 0.048 \left( \frac{f_{cm}^{2/3}}{E_{fu} \rho_f} \right)^{0.47} \quad \varepsilon_{fu} = 0.048 \left( \frac{21^{2/3}}{230000 \times 0.003} \right)^{0.47} = 0.0058 \quad (\text{FIB, 5-4a})$$

$$\varepsilon_{fk,e} = k \varepsilon_{f,e} = 0.8 \times 0.0058 = 0.0046 \quad (\text{FIB, 5-3})$$



$$\varepsilon_{fd,e} = \varepsilon_{fk,e} / \gamma_f = 0.0046 / 1.35 = 0.0034$$

where,  $\varepsilon_{fd,e}$  is the design value of effective FRP strain,  $b_w$ , is the minimum width of cross section over the effective depth,  $d$ , is the effective depth of cross section,  $\rho_f$ , is FRP reinforcement ratio,  $E_{fu}$ , is the elastic modulus of FRP in the principal fibre orientation,  $\theta$ , is the angle of diagonal crack with respect to the member axis, assumed equal to  $45^\circ$  and  $\alpha$ , is the angle between principal fibre orientation and longitudinal axis of member.

Use of CFRP wrapping system increases the design shear capacity of the strengthened member by 310 kN and 323 kN based on the FIB and ACI design guidelines respectively. The results indicated that both the guidelines predict almost the same shear capacity increases using the complete wrapping scheme for strengthening of the headstock. The CFRP shear reinforcement is considered as contact critical shear reinforcement. Hence the ultimate failure does not occur with de-bonding.

## 6.6 Other issues

The ACI guideline suggested imposing reasonable strengthening limits to guard the strengthened member against failure of the FRP strengthening system and collapse of the structure due to fire, vandalism, or other causes. It is recommended that the existing strength of the structure be sufficient to a level of load as described by below Equation 2.

$$(\phi R_n)_{existing} \geq (1.2S_{DL} + 0.85S_{LL})_{new} \quad (\text{ACI 440, 8-1})$$

where  $S_{DL}$  is dead load and  $S_{LL}$  is live load. It is also recommended that the strength of a structural member with a fire-resistance rating before strengthening should satisfy the conditions of Equation 3.

$$(R_{n\theta})_{existing} \geq S_{DL} + S_{LL} \quad (\text{ACI 440, 8-2})$$

$(R_{n\theta})_{existing}$  is the nominal resistance of the member at an elevated temperature, which can be determined using the ACI 216R guideline.

Environmental conditions affect the performances of the FRP system. The mechanical properties of FRP systems degrade under exposure to certain environments, such as alkalinity, salt water, chemicals, ultraviolet light, high temperatures, high humidity and freezing and thawing cycles. The ACI guideline account for this degradation using the environmental reduction factor for the design material properties of CFRP as described in section 5.4.1.

The FIB guideline recommends the accident design verification to prevent failure of the FRP strengthening system and collapse of the structure due to fire, vandalism, or other causes. The existing member is subjected to all relevant accidental load combinations of the strengthened member. The verification is the performance in the ultimate limit state, considering the partial safety factors of 1.0 and considering partial safety coefficients and combination factors using Eurocode 1 (EC1), Part 1 (CEN 1994). The FIB guideline also recommends that sufficient attention should be paid to the special design aspects, as they can have a considerable influence on the structural safety.

The existing structural strength of the headstock was checked to be sufficient to satisfy the ACI and FIB guidelines requirements in the accidental design situation. The existing structure has not been rated for fire-resistance; hence it was not checked for Equation ACI 440, 8-2.

## **6.7 Comparison of the provisions of the two major guidelines: ACI and FIB**

Following conclusions can be made based on the work reported in chapter 6.

- Both design guidelines adopt the same principal of design to estimate shear and flexural capacity enhancements of the strengthened member.
- The ACI guideline is more conservative in prediction of flexural capacity enhancement for the strengthened headstock. This is mainly due to the use of an additional strength reduction factor of 0.85 applied to the contribution of FRP reinforcement.
- The FIB guideline uses a more accurate approach to check de-bonding of FRP laminates from the concrete substrate, which covers all possible bond failure modes.
- Both design guidelines predicted almost the same shear capacity enhancement for the strengthened member.

In view of above finding, it may be concluded that the use of ACI 440 design guideline may be more appropriate for FRP strengthening applications in Australia. The design concepts and philosophy used by ACI is similar to those adopted by AS3600 (2002). However, in considering the failure of FRP composites in de-bonding and anchorage zones, use of FIB appears to be more appropriate since it systematically covers all possible scenarios incorporating more recent research findings.

## **6.8 Summary of FRP strengthening scheme**

The design of FRP strengthening system for the Tenthill bridge headstock can be summarized as follows:

- The flexural strength of the headstock can be increased from 3800 kN-m to 5854 kN-m by bonding four FRP strips of 120 x 1.4 mm to the tension face of the beam section (bottom fibre) of the headstock with fibres oriented along the length of the member ( Figure 6-5).
- The shear strength of the headstock can be increased from 2065 kN to 2711 kN by complete wrapping of the beam with carbon fibres oriented along the transverse axis of the beam section (Figure 6-6).

Figure 6-5 Flexural strengthening scheme

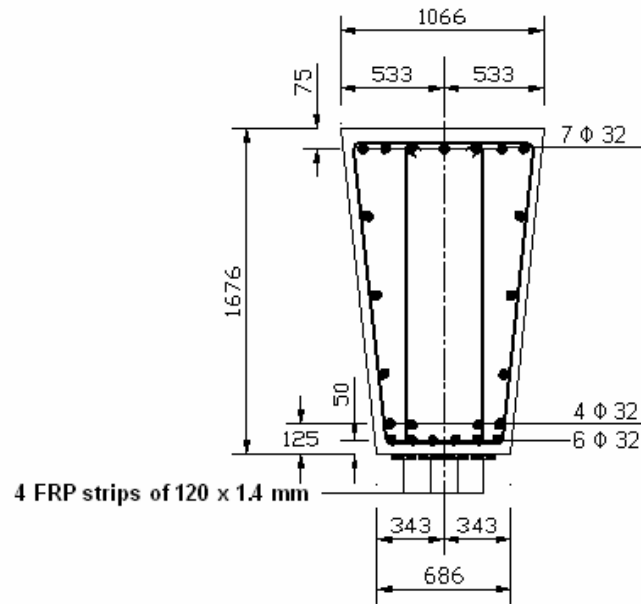
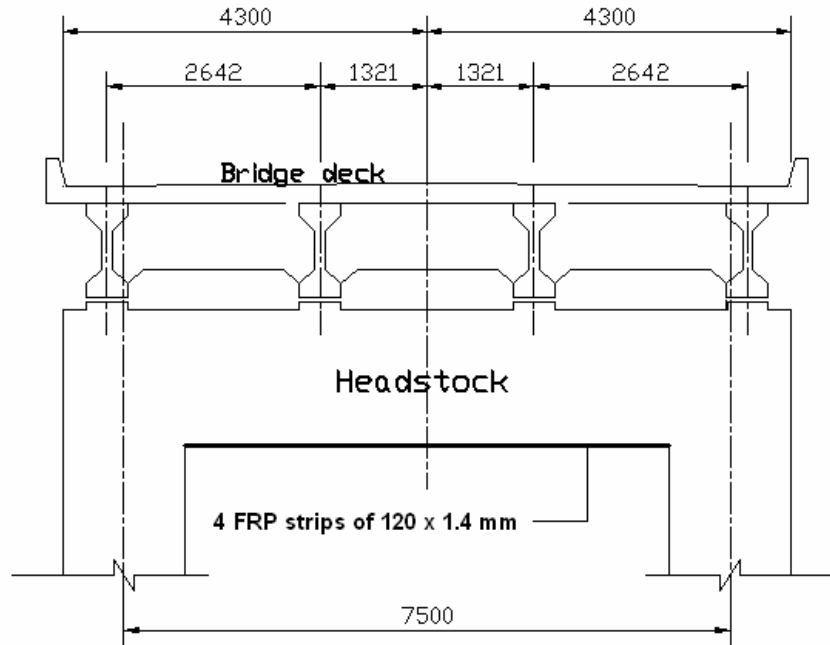
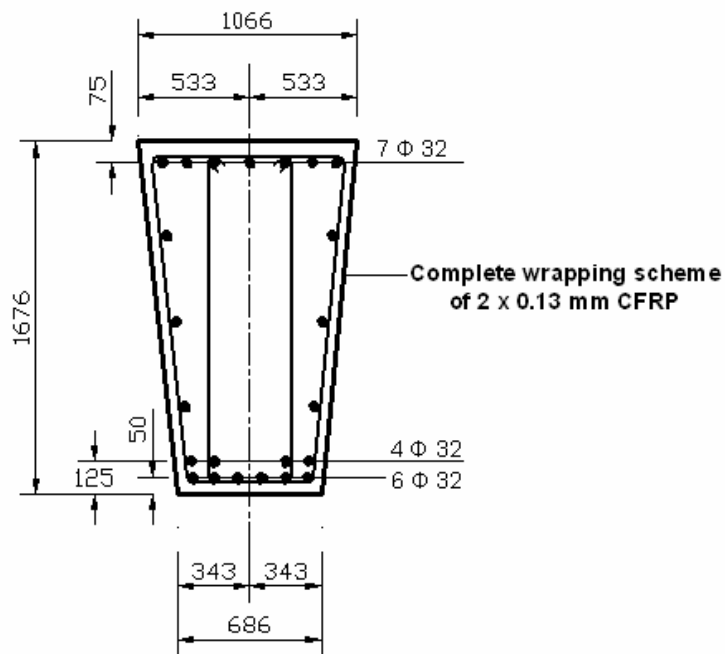
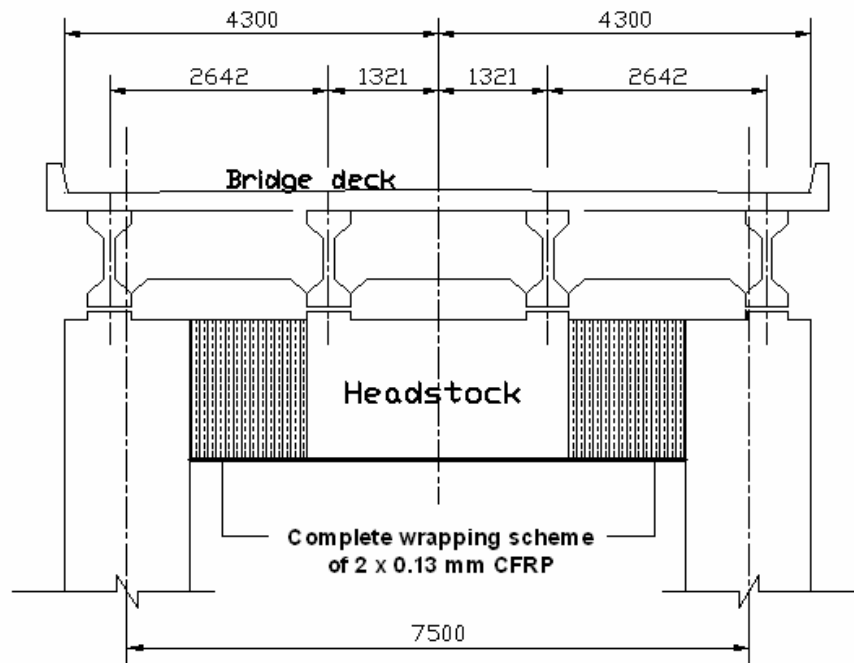


Figure 6-6 Shear strengthening scheme



## **7 COMPARISON OF POST TENSIONING AND FRP STRENGTHENING**

The structures division of QDMR (Ms. Louise Chandler) has developed a solution for rehabilitation of the bridge structure using external post-tensioning. The research team has re-assessed the proposed scheme and has developed a scheme utilising FRP composites available in the market. This chapter presents a comparison between these two strengthening solutions.

### **7.1 Flexural Strengthening**

The design bending moment capacity for the FRP strengthening system was calculated based on the two design guidelines of ACI 440 and FIB 14. The design bending moment capacity of 6720 kN-m and 5854 kN-m were calculated for strengthened section based on the FIB and ACI design guidelines respectively. The calculated moment capacities using the two design guidelines indicated that the predicted capacity enhancement based on the ACI guideline is more conservative. Therefore it was decided to use the flexural capacity of 5854 kN-m as a result of FRP strengthening system.

The design flexural capacity of 6273 kN-m was calculated for post-tensioning strengthening system in accordance with code based calculations (QDMR calculations). However it may be concluded that the both strengthening systems would increase the capacity of the headstock to the adequate level of the ultimate strength.

### **7.2 Shear Strengthening**

Due to the observed shear cracks, the shear strengthening of the headstock is the main concern in design of the strengthening system.

Pre-stressing has a significant influence on the load capacity in flexural shear and shear in diagonal cracking of a pre-stressed member. The flexural and inclined crack formation can be delayed with the horizontal component of pre-stressing force. The vertical component of the pre-stressing force affects the shear force acting on concrete. Shear capacity after post-tensioning strengthening was checked at both flexural-shear cracking and web shear cracking. The post-tensioning strengthening system increases the shear capacity by approximately 400 kN based on code provisions for an un-cracked beam. However, literature review shows that the shear strength of a beam after crack initiation decreases by 10-25% (Duthinh, 1999).

The shear strength of a reinforced concrete or a pre-stressed concrete beam after initiation of the shear cracks mostly come from two mechanisms of the aggregate interlock and shear friction across shear cracks. The importance of these mechanisms has been recognized for quite some time. However, neither beam-design equations for shear (Austroads Bridge design code (1992)) nor the equations in AS3600 (2000) explicitly account for shear friction and aggregate interlock. Therefore caution must be used in estimating the shear strength of the cracked reinforced concrete beams. In last two decades, more rational methods have been developed to explicitly account for the contribution of shear friction across shear cracks and aggregate interlock in shear strength calculation. The shear strength of reinforced concrete and prestressed concrete (post-tensioned) beams remains an active area of

research (Duthinh 1999). The ultimate shear strength of cracked section can be estimated by reducing the nominal shear strength of un-cracked section by 15%.

The design for shear strengthening of a reinforced concrete member in FRP strengthening system is based on truss model and superposition principle with some considerations for the orthotropic behaviour of the CFRP material. The shear strength of a strengthened member is determined by adding the contribution of the CFRP reinforcing to the contributions from the concrete and shear reinforcement. Use of a layer of 0.13 mm thick CFRP wrapping system increases the design shear capacity of the strengthened member by 323 kN based on the ACI design guideline. The design shear capacity of the headstock can be increased to the desired level of ultimate shear strength by using of 2 layers of 0.13 mm thick CFRP wrapping system. Hence FRP strengthening would compensate for the reduction of shear capacity due to existing shear crack in the beam.

### **7.3 Conclusions**

The comparison of the strengthening method of FRP system and post-tensioning system shows that the both methods can be used to increase the design flexural capacity of the headstock to the adequate level of ultimate strength. Main Roads primary requirement was to close the shear crack with prestress to ensure long term durability, and then check that the shear design is adequate, given the bridge has now been bypassed and is not on the main heavy load route west of Brisbane. Main Roads calculated a capacity of about 90% of HLP 320 which is consistent with other older bridges on the road link. It is possible to gain increased shear capacity using FRP composites if this was necessary for an older bridge on a heavy load route. The beam-design equations for shear in AS3600 (2000) nor Austroad Bridges design code cannot be also used to estimate the shear strength of the cracked reinforced concrete beams. Therefore use of post-tensioning strengthening system is not recommended for shear strengthening of the headstock.

The FRP strengthening system may be used to increase the design shear capacity of the headstock to the adequate level of ultimate shear strength.

## 8 CONCLUSIONS

Work reported herein was aimed at developing a strengthening solution for reinforced concrete bridge beams in shear and flexure using innovative FRP technology, with the strategic goal of identifying decisions made by the designer at various stages of the process. In achieving the goal, research has been conducted covering a complete review of the capacity assessment of the structure, analysis of a traditional strengthening solution using external post-tensioning and developing an FRP solution using two international guidelines and published research in conjunction with the Austroads bridge design code (1992)

Condition assessment of the structure is the first step in determining the rehabilitation methodology. Clear identification of the performance level needed and deficiencies require design load definition, definition of traffic, material properties and design documentation of the existing structure (Nezamian et al. 2004). The headstock condition assessment is presented in Chapters 2, 3 and 4. It may be concluded that the shear and flexural strengthening of the headstock is required due to the inadequate shear and flexural capacities of the existing cross section. Further it is noted that current provisions of design standards around the world do not cover calculation of the residual shear capacity of a reinforced concrete beam cracked in shear. Published literature (Duthinh (1999)) indicates that the residual shear capacity of a reinforced concrete beam with a diagonal shear crack can be less than the shear strength of an uncracked reinforced concrete beam by about 15%.

A typical strengthening scheme using external post-tensioning is presented in chapter 5. The solution has been developed by QDMR and checked and presented by the research team to enable a comparison. It is noted that large post tensioning loads could initiate sliding failure in a beam with a shear crack. An upper limit on the pre-stress force needs to be established to prevent this. No published research work could be found which covers this phenomenon. The applied prestress load in this case was relatively small in comparison to the compression stress limits.

A comparison between the recommendations of two design guidelines of the ACI 440 and the FIB 14 in design of externally bonded FRP systems to strengthen the headstock is outlined in Chapter 6. The following conclusions can be drawn from the comparison.

- Both design guidelines adopt the same principal of design to estimate shear and flexural capacity enhancements of the strengthened member.
- The ACI guideline is more conservative in prediction of flexural capacity enhancement for the strengthened headstock. This is mainly due to the use of an additional strength reduction factor of 0.85 applied to the contribution of FRP reinforcement.
- The FIB guideline uses a more accurate approach to check de-bonding of FRP laminates from the concrete substrate, which covers all possible bond failure modes.
- Both design guidelines predicted almost the same shear capacity enhancement for the strengthened member.

In view of above findings, it may be concluded that the use of ACI 440 design guideline may be more appropriate for FRP strengthening applications in Australia. The design concepts and philosophy used by ACI is similar to those adopted by AS3600 (2002). However, in considering the failure of FRP composites in de-bonding and anchorage zones, use of FIB to check debonding (section 6.4.4) appears to be more appropriate since it systematically covers all possible scenarios.

The comparison of the strengthening methods of FRP system and post-tensioning system is presented in Chapter 7. The following conclusions may be made:

- Both methods can be used to increase the design flexural capacity of the headstock to the adequate level of ultimate strength.
- The post-tensioning solution will increase the design shear capacity of the headstock to that of a PSC member with the original shear steel.
- In this study it was possible to achieve a design capacity sufficient for HLP 320 design loads.
- Neither the beam-design equations for shear in AS3600 (2000) nor Austroad Bridges design code (1992) can be used to estimate the shear strength of the cracked reinforced concrete beams.
- The FRP strengthening system which adds more “shear reinforcement” may be used to increase the design shear capacity of the headstock if this is required (i.e. original design deficient in shear).



## 9 REFERENCES

- ACI 216R, "Guide for Determining the Fire Endurance of Concrete Elements"
- ACI 318-99 (1999). "Building Code Requirements for Structural Concrete and Commentary"
- American Concrete Institute Committee 440, (2002). "Guide for the design and construction of externally bonded FRP systems for strengthening concrete structures"
- AS3600 (1988), "Concrete Structures", Australian Standard, Standards Association, Australia,
- Austrroads (1992), "Bridge design code", Section 2: Design loads
- Carse, A. (1996), "The asset management of alkali-silica reaction in a long bridge structure" *Proceeding 10<sup>th</sup> Int. Conference on AAR in concrete*, Australia pp. 1023-1032.
- CEN (1994), *Eurocode 1: Basis of design and actions on structures – Part 1: Basis of design*. ENV 1991-1, Comité Européen de Normalisation, Brussels, Belgium.
- Duthinh, D. (1999). "Sensitivity of Shear Strength of Reinforced Concrete and Prestressed Concrete Beams to Shear Friction and Concrete Softening According to Modified Compression Field Theory" *ACI Structural Journal*, V96 No. 4 pp. 495-508
- Fenwick, J. M., and Rotolone, P., (2003). "Risk Management to Ensure Long Term Performance in Civil Infrastructure" *21st Biennial Conference of the concrete institute of Australia*, Brisbane, Australia, pp. 647-656
- GangRao, H.V.S., and Vijay, P.V. (1998) "Bending Behavior of Concrete Beams Wrapped with Carbon Fabric" *Journal of Structural Engineering*, V.124, No.1, pp. 3-10
- Holzenkämpfer, P. (1994), *Ingenieurmodelle des verbundes geklebter bewehrung für betonbauteile*. Dissertation, TU Braunschweig (In German).
- Kalra, R. and Neubauer, U. (2003). "Strengthening of the Westgate Bridge with Carbon Fibre Composites - A Proof Engineer's Perspective" *21st Biennial Conference of the concrete institute of Australia*, Brisbane, Australia, pp. 245-254
- Neubauer, U. and Rostásy, F. S. (1997), Design aspects of concrete structures strengthened with externally bonded CFRP-plates. In *Concrete+Composites, Proceedings of the 7th International Conference on Structural Faults and Repair*, 2, 109-118.
- Nezamian, A., Setunge, S., Kumar, A. (2004). "Decision Support in Using Fiber Reinforced Polymer (FRP) composites in Rehabilitation of Concrete Bridge Structures" *Proceeding of Innovative Materials and Technologies for Construction and Restoration*, June 6-9, 2004, Lecce, Italy
- Niedermeier, R. (2000), *Zugkraftdeckung bei klebarmierten bauteilen (Envelope line of tensile forces while using externally bonded reinforcement)*. Doctoral Dissertation, TU München, (In German).
- Nystrom, H. E., Walkins, S. E., Nanni, A., and Murray, S. (2003). "Financial Viability of Fiber-Reinforced Polymer (FRP) Bridges" *Journal of Management in Engineering*, Vol. 19 No. 1 pp. 2-8
- Sika Australia Pty Limited "Heavy-Duty CFRP strengthening system" Product Guide Specification, February 2004. Web site: <http://www.sika.com.au>
- Täljsten, B. (1999 a), Förstärkning av befintliga betongkonstruktioner med kolfiberväv eller laminat, Dimensionering, material och utförande. *Technical Report 1999:12*, LuleaUniversity of Technology (In Swedish).

- Täljsten, B. (1999 b), Strengthening of existing concrete structures with carbon fibre fabrics or laminates. Design, material and execution. *Extract from Swedish National Railroad and Road Codes*.
- The international federation for structural concrete (CEB-FIB), technical report bulletin 14 (2002). "Externally bonded FRP reinforcement for RC structures"
- Triantafillou, T. C. (1998), "Shear strengthening of reinforced concrete beams using epoxy bonded FRP composites" *ACI Structural Journal*, **95**(2), 107-115.
- Shepherd, B. and Sarkady, A. (2002) "Carbon Fibre Fabric Strengthening of Little River Bridge" *Proc. IABSE Symposium, Melbourne Australia*, Sept 11-13, 2002

## 10. NOTATION

$A$	= cross-sectional area of a member (mm <sup>2</sup> )
$A_{fv}$	= total area of FRP shear reinforcement (mm <sup>2</sup> )
$A_f$	= total area of FRP reinforcement (mm <sup>2</sup> )
$A_{s1}$	= total area of tensile longitudinal reinforcement (mm <sup>2</sup> )
$A_{s2}$	= total area of compressive longitudinal reinforcement (mm <sup>2</sup> )
$A_{st}$	= total area of longitudinal reinforcement (mm <sup>2</sup> )
$A_{sv}$	= the cross-sectional area of shear reinforcement (mm <sup>2</sup> )
$a_v$	= a distance from the face of the nearest support
$b$	= average width at the cross section
$b_f$	= width of FRP reinforcement
$C_E$	= environmental reduction factors
$c_f$	= factor relating the concrete fracture energy to the mean tensile strength
$d$	= distance from extreme compression fiber to the centroid of the non prestressed steel tension reinforcement (mm)
$d_p$	= distance from extreme compression fiber to the centroid of the prestressed tendons
$E_c$	= modulus of elasticity of the concrete (MPa)
$E_f$	= modulus of elasticity of FRP (MPa)
$E_s$	= modulus of elasticity of reinforcement steel (MPa)
$f'_c$	= specified compressive strength of concrete (MPa)
$f_{cbd}$	= design bond shear strength of concrete (MPa)
$f_{cd}$	= design value of the concrete compressive strength (MPa)
$f_{ck}$	= characteristic value of the concrete compressive strength (MPa)
$f_{ctk}$	= characteristic value of the concrete tensile strength (MPa)
$f_{ctm}$	= mean value of the concrete tensile strength (MPa)
$F_{py}$	= prestress force
$f_{sy}$	= specified yield strength of non prestressed steel reinforcement (MPa)
$f_{sy:f}$	= the yield strength of shear reinforcement (MPa)
$f_{yd}$	= design value of the steel yield strength (MPa)
$h$	= total depth of the member
$I$	= a second moment area of a member (mm <sup>4</sup> )
$I_{cs}$	= moment of inertia of transformed cracked section after strengthening (mm <sup>4</sup> )
$I_{co}$	= moment of inertia of transformed cracked section before strengthening (mm <sup>4</sup> )
$k_b$	= size factor
$k_c$	= concrete compaction factor
$M^*$	= applied moment at the section (kN-m)

$\max \Delta \sigma_{fd}$	= design value of maximum possible increase in FRP tensile stress between two subsequent cracks (MPa)
$M_{cr}$	= cracking moment
$M_o$	= acting moment during strengthening (kN-m)
$M_o$	= the decompression moment
$M_{Rd}$	= resisting design moment
$M_u$	= factored moment at section (kN-m)
$P_e$	= the prestressing force (N)
$P_v$	= the vertical component of the prestressing force (N)
$Q$	= the first moment of area of a member ( $\text{mm}^3$ )
$R_n$	= nominal strength of member
$R_{n\theta}$	= nominal strength of member subjected to the elevated temperature associated with a fire
$S_{DL}$	= dead load effect
$S_f$	= maximum spacing of FRP
$S_{LL}$	= Live load effect
$s_{sm}$	= mean bond stress of the steel reinforcement
$t_f$	= nominal thickness of the FRP reinforcement (mm)
$V^*$	= applied shear force at the section (kN)
$V_f$	= nominal shear strength provided by FRP reinforcement (N)
$V_n$	= nominal shear strength (N)
$V_o$	= the shear force which would occur at a section when the bending moment at the section was equal to decompression moment (N)
$V_{Rd}$	= design resisting shear
$V_t$	= a shear force producing principle tensile stress (N)
$V_u$	= required shear strength based on factored loads (N)
$V_{uc}$	= nominal shear strength provided by concrete with steel flexural reinforcement (N)
$V_{us}$	= nominal shear strength provided by steel stirrups (N)
$w_f$	= width of FRP reinforcing plies (mm)
$x$	= depth of the compression zone
$Z$	= the first moment of area of an uncracked cross-section ( $\text{mm}^3$ )
$z_m$	= mean lever arm of internal forces
$\alpha$	= an assumed value for the depth of the line of action of the resultant compressive force
$\alpha_f$	= modular ratio for non-prestressed steel
$\beta$	= a coefficient with or without numerical subscript
$\delta_G$	= stress block centroid coefficient
$\epsilon_{co}$	= initial concrete strain in the extreme compressive fiber before strengthening, or unconfined concrete strain at peak stress
$\epsilon_{cu}$	= ultimate concrete strain
$\epsilon_f$	= FRP strain
$\epsilon_{fd,e}$	= design value of effective FRP strain
$\epsilon_{fe}$	= effective FRP strain
$\epsilon_{fk,e}$	= characteristic value of effective FRP strain
$\epsilon_{fu}$	= ultimate FRP strain
$\epsilon_o$	= initial strain at the extreme tensile fiber before strengthening
$\epsilon_{s1}$	= tensile steel strain
$\epsilon_{s2}$	= compressive steel strain
$\epsilon_{yd}$	= design value of the yield strain of the steel reinforcement
$\phi$	= strength-reduction factor

$\gamma$	= multiplier to determine the intensity of an equivalent rectangular stress distribution for concrete
$\gamma_M$	= partial safety factor for the materials
$\gamma_{mfrp}$	= material safety factor for the FRP
$\gamma_{ms}$	= material safety factor for the steel reinforcement
$\gamma_{mc}$	= material safety factor for the concrete
$\kappa_m$	= bond dependant coefficient for flexure
$\theta_v$	= the angle between the concrete compression struts and the longitudinal axis of the member used in calculating shear strength of a beam
$\rho_f$	= ratio of FRP reinforcement
$\rho_s$	= ratio of non-prestressed reinforcement
$\sigma_1$	= the principal stress of effective prestress force in the concrete (MPa)
$\sigma$	= the average compressive stress of effective prestress force in the concrete (MPa)
$\sigma_{fd}$	= design value of FRP stress (MPa)
$\tau_{fm}$	= mean bond stress of the FRP
$\tau_{sm}$	= mean bond stress of the steel reinforcement
$\tau$	= the shear stress effective prestress force in the concrete (MPa)
$\psi$	= stress block area coefficient
$\psi_f$	= FRP strength reduction factor

## 11. AUTHOR BIOGRAPHIES

### Dr Abe Nezamian,

**Education:** PhD, Monash University, Australia 2003, B.Sc. (Hons) Azad University, Iran 1990

**Professional Experience:** Nine years of experience in consulting engineering companies.

**Research Interests:** Rehabilitation of aged concrete structures, composite structures, and concrete filled tubular steel columns

### Dr Sujeeva Setunge,

**Education:** PhD, Monash University, Australia (1993), B.Sc. Eng.(Hons) Sri Lanka (1985)

**Professional Experience:** 1 year in Civil Engineering Construction and 15 years in Academia.

**Research Interests:** Infrastructure asset management, creep and shrinkage of concrete, innovative construction materials and composites, high strength and high performance concrete